Prepublished Copy

NATURE ENVIRONMENT AND POLLUTION TECHNOLOGY

Article In Press

PEER-REVIEWED PREPUBLISHED MANUSCRIPT

This is a peer-reviewed prepublished version of the paper to be published in **Vol. 26, No. 1, March 2027.**

Urban Expansion and Green Cover Loss in Hyderabad, India: Sentinel 2 Based LULC Analysis and MLP–Markov Urban Growth Modeling

Shaik Habeeb Ahmed, Shashikanth Kulkarni, Harish Gupta and Amey Pathak

RECEIVED
13 June 2026

CITE THIS ARTICLE
Ahmed, S.H., Kulkarni, S., Gupta, H. and Pathak, A., 2027. Urban Expansion and Green Cover Loss in Hyderabad, India: Sentinel 2 Based LULC Analysis and MLP–Markov Urban Growth Modeling. *Nature Environment and Pollution Technology*, 26(1), B4462.

https://doi.org/10.46488/NEPT.2027.v26i01.B4462

EARLY-ACCESS STATEMENT

This manuscript, after peer review, is being released online in its original, unedited form to provide early access to its findings. Prior to final publication, it will undergo additional editing and formatting. Readers may note that, as an unedited version, the manuscript may have linguistic and other minor errors. The DOI will be active after the final publication of the paper.

PUBLICATION STATUS

PEER REVIEW	ONLINE VERSION	FINAL ISSUE
Completed	**Prepublished**	**March 2027**

Urban Expansion and Green Cover Loss in Hyderabad, India: Sentinel 2 Based LULC Analysis and MLP–Markov Urban Growth Modeling

Shaik Habeeb Ahmed[1] , Shashikanth Kulkarni[1]† , Harish Gupta[1], Amey Pathak[2]

[1]Dept. of Civil Engineering, University College of Engineering (A), Osmania University, Hyderabad, India;

skhabeeb145@gmail.com, kulkarni.shashikanth@osmania.ac.in, harishgupta78@osmania.ac.in

[2]Food and Agriculture Department, Indian Institute of Technology, Kharagpur, India-; amey@agfe.iitkgp.ac.in

†Corresponding author: Shashikanth Kulkarni; **kulkarni.shashikanth@osmania.ac.in**

ORCID: **https://orcid.org/0000-0001-7481-649X**

Abstract

The present study analyses land use and land cover (LULC) dynamics and urban growth in Hyderabad, India, using multi-temporal Sentinel 2 imagery and a multilayer perceptron–Markov chain (MLP–MC) modelling framework. Sentinel 2 Level 1C data for 2018, 2020, and 2022 were pre-processed and classified into four LULC classes—water, green infrastructure, built-up, and barren land—using supervised maximum likelihood classification, achieving overall accuracies of 94.8%, 94.7% and 96.3% and kappa coefficients of 0.92, 0.90, and 0.93, respectively. Change analysis within the Outer Ring Road (ORR) revealed a substantial increase in built-up area from 844.36 km² (57.81%) in 2018 to 948.95 km² (64.97%) in 2022, primarily at the expense of green infrastructure, which declined from 301.04 km² (20.61%) to 173.45 km² (11.87%); the dominant transitions were green infrastructure built-up (8.74% of total area) and barren land to built-up (2.3%). Urban growth was modeled in the Land Change Modeler (TerrSet) by deriving transition potential maps using an MLP with distance to roads, distance to existing built-up areas, and distance to ORR as driving factors, and by coupling these with Markov chain analysis to simulate future LULC. Model validation against the observed 2022 LULC produced kappa values of 84.98% (K_standard), 87.83% (K_no), and 89.01% (K_location), and a built-up prediction accuracy of 98.6%, indicating strong agreement in both quantity and spatial allocation. The validated model was then used to project LULC scenarios for 2030, 2040, and 2050, showing built-up areas potentially expanding to 1135.46 km² (77.73%) by 2030 and exceeding 90% of the ORR region by 2050,

Keywords: Landuse Land cover 1; Urban Growth Modeling 2; ANN 3 Sentinel 2

1. INTRODUCTION

Urbanization is a dynamic and multi scalar process that restructures cities both horizontally and vertically, due to population progress, industrialization, infrastructure expansion, and broader socio economic transformations (Ramachandra et al., 2012a: Wang et al., 2013). Land use and land cover (LULC) change indicates the visible signs of this process, influencing ecosystem services, surface energy balance, hydrology, and the spatial distribution of human activities, with urban areas often exhibiting rapid, non-linear changes over relatively short time intervals (Weng, 2001; Jieli et al., 2010). In fast growing metropolitan regions, understanding the rates, patterns, and drivers of LULC change is essential for sustainable land use planning, risk informed infrastructure development, and evidence based environmental policy formulation (Soffianian et al., 2010; Talukdar et al., 2020; Kumar et al 2025).

2. BACKGROUND RESEARCH (REVIEW OF LITERATURE)

Remote sensing and Geographic Information Systems (GIS) are the latest and emerging technologies for observing LULC change because they provide synoptic, repeatable, and multi spectral observations over large areas and long time periods (Lillesand et al., 2004; Jeanne et al., 2002). Medium- to high-resolution satellite data enable the mapping of urban land cover classes and the detection of temporal change, while classification methods such as the maximum likelihood classifier have been widely used to derive reliable thematic maps across different epochs (Anderson et al., 1976; Ramachandra et al., 2012b). Sentinel 2, as part of the Copernicus programme, offers 10–20 m multi-spectral imagery that is particularly suited for detailed urban LULC mapping and change analysis, thereby providing a robust empirical basis for calibrating and validating urban growth models.

To move beyond descriptive mapping, a range of spatially explicit modelling frameworks has been developed to simulate urban expansion and project future land-use patterns. Cellular Automata (CA) and Markov chain models are frequently employed to represent spatial contiguity and temporal transition probabilities, respectively, and their integration (CA–Markov) has been shown to capture key characteristics of urban sprawl in diverse settings (Guan et al., 2011; Jokar et al., 2013; Khawaldah et al., 2020; Mansour et al., 2020). More recently, Artificial Neural Networks (ANN), including multilayer perceptrons (MLP), have been incorporated into CA–Markov frameworks to better represent complex, non linear relationships between LULC transitions and driving factors such as proximity to roads, existing built up areas, and socio economic variables (Maithani, 2009; Megahed et al., 2015; Guo et al., 2020; Zhang, 2016). Comparative assessments indicate that ANN based CA–Markov models can outperform traditional approaches in terms of predictive accuracy when appropriately trained and validated (Talukdar et al., 2020).

In the Indian context, several studies have applied remote sensing and CA/ANN based models to investigate urban growth and its environmental implications in cities such as Bangalore, Bhubaneswar, Cairo like megacities, and others (Ramachandra et al., 2012; Aithal et al., 2013; Pathy and Panda, 2012; Megahed et al., 2015). These works collectively highlight the rapid conversion of agricultural and peri urban land to built up areas, the loss of vegetation and water bodies, and emerging challenges related to flooding, urban heat islands, and degradation of ecological corridors. However, for Hyderabad—one of India's major IT and service hubs and the capital of Telangana—there is still relatively limited literature that simultaneously exploits recent high resolution Sentinel-2 data and systematically calibrated MLP–Markov chain models for urban growth prediction. Given the city's accelerated expansion within and around the Outer Ring Road (ORR), and the associated transformation of green infrastructure and barren land into urban settlements, there is a pressing need for robust, spatially explicit LULC assessments and scenario based projections to support sustainable planning and management.

Against this backdrop, the present study focuses on urban growth modelling of Hyderabad city, India, using multi temporal Sentinel-2 imagery and a multilayer perceptron–Markov chain (MLP–MC) framework implemented in the Land Change Modeler (LCM) of IDRISI TerrSet. By integrating remote sensing derived LULC maps with proximity based driving factors (e.g., distance to roads and existing built up areas), the study aims to quantify recent LULC dynamics between 2018 and 2022 and to simulate future land use configurations up to 2050, thereby contributing both to the methodological literature on ANN based CA–Markov models and to the practical needs of urban planners and policymakers in Hyderabad.

The objectives of this study are to generate accurate LULC maps of Hyderabad city for the years 2018, 2020, and 2022 from Sentinel-2 satellite imagery using supervised maximum likelihood classification, and to assess their thematic accuracy using confusion matrices and kappa statistics. A second objective is to quantify the spatio-temporal dynamics of major LULC classes (water, green infrastructure, built-up, and barren land) within the Outer Ring Road (ORR) corridor, and to identify the dominant transitions contributing to urban expansion during 2018–2022. The study further aims to develop and calibrate a MLP–MC urban growth model in the LCM environment by deriving transition potential maps based on key driving factors such as distance to roads and existing urban areas. Model validation constitutes another key objective, achieved by comparing the simulated 2022 LULC map with the observed 2022 map using visual analysis and kappa variants (K_standard, K_no, K_location). Finally, the validated model will be applied to project future LULC scenarios for 2030, 2040, and 2050, with a discussion of the implications of predicted urban growth for green infrastructure preservation, environmental sustainability, and urban planning in Hyderabad.

3. MATERIALS AND METHODS

3.1 **STUDY AREA:-**Hyderabad, the capital of Telangana state in South India, serves as the primary study area for this investigation. The city lies between latitudes 17°18′ N and 17°35′ N and longitudes 78°15′ E and 78°40′ E, encompassing an area of approximately 1460 km² within the Outer Ring Road (ORR) boundary, which spans 158 km and encircles key urban nodes including HITEC City, the Financial District, and Rajiv Gandhi International Airport. Developed along the banks of the Musi River—a tributary of the Krishna—the city sits at an average elevation of 542 m above mean sea level. It includes prominent man-made lakes such as Hussain Sagar, Himayat Sagar, and Osman Sagar (Fig. 1).

.

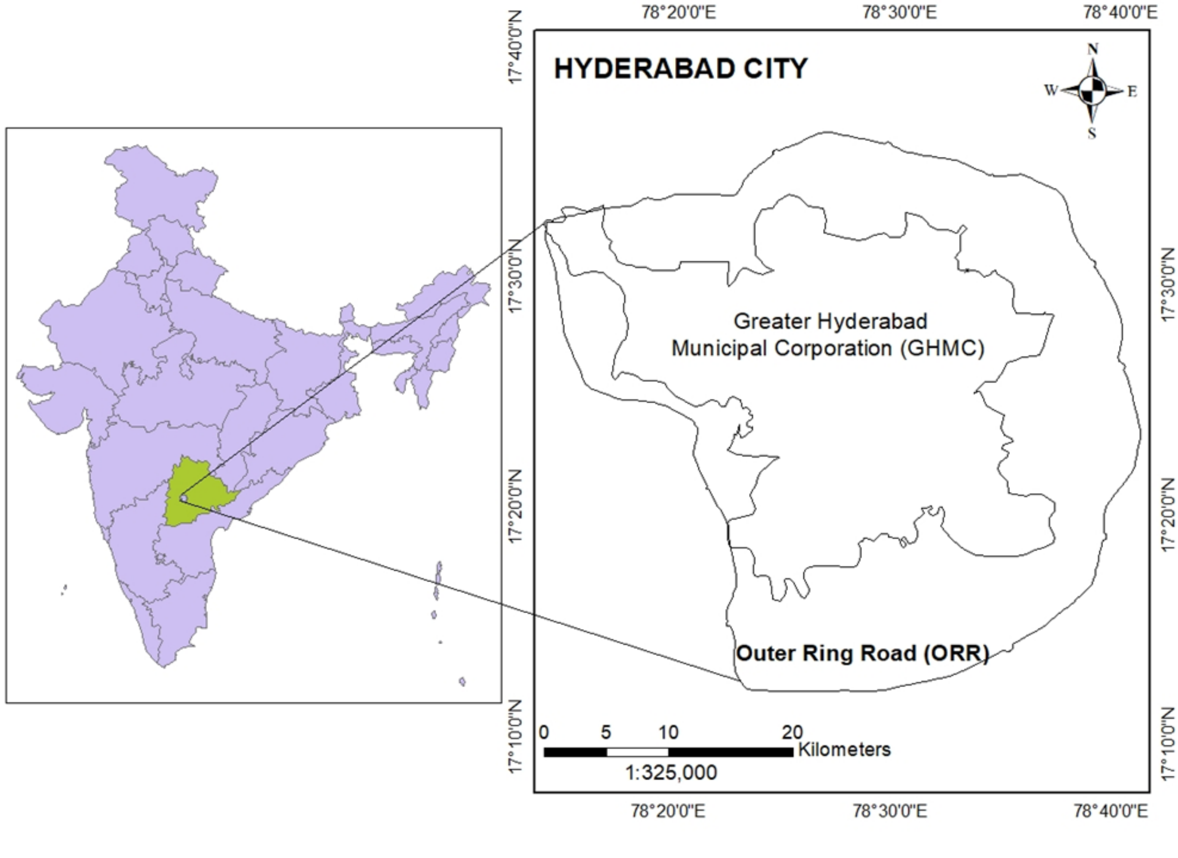

Figure 1 Location map of the study area

GHMC (Greater Hyderabad Municipal Corporation) area forms the urban core, while peri-urban zones in Ranga Reddy district extend toward the ORR, which features 20 major interchanges connecting radial highways like NH-44, NH-65, and SH-1. This configuration supports rapid connectivity but also facilitates outward urban sprawl, with new settlements emerging near junctions such as Gachibowli, Nanakramguda, Shamshabad, and Pedda Amberpet. The ORR delineates the study boundary, focusing analysis on densely developed zones within this perimeter, where LULC transitions are most pronounced.

With a 2011 census population of 6.9 million—now estimated higher due to ongoing migration—Hyderabad ranks among India's top metropolitan areas, driven by the IT, pharmaceuticals, and services sectors, which intensify pressure on land resources. The region's semi-arid climate, characterized by hot summers and moderate monsoons, combined with expanding built-up cover, heightens vulnerabilities to urban flooding, heat islands, and water stress, making LULC monitoring critical for resilience planning. Figure 1 illustrates the ORR alignment relative to GHMC limits and major landmarks.

3.1 DATA ACQUISITION AND PREPARATION

Multi-temporal Sentinel-2 Level-1C imagery at 10 m spatial resolution was acquired from the Copernicus Open Access Hub for the years 2018, 2020, and 2022, covering the Hyderabad ORR region. Cloud-free (0% cloud cover) dry-season images were selected to minimize atmospheric interference and ensure consistent phenological conditions across acquisition dates, with path/row coverage spanning tiles T43QDM and T43QDN. Detailed acquisition parameters are summarized in Table 1.

Pre-processing followed a standard workflow in QGIS 3.28 and Semi-Automatic Classification Plugin (SCP): (i) atmospheric correction using Sen2C or to derive Level-2A surface reflectance products; (ii) clipping to the ORR administrative boundary vector (sourced from HMDA); (iii) band stacking of relevant bands (B2, B3, B4, B8, B11, B12) for classification; and (iv) resampling to 10 m resolution where needed. Ancillary data included the 2022 road network vector (OpenStreetMap) and the existing built-up layer (derived from 2022 LULC) for driving factor generation.

Table 1 Sentinel 2 used for land cover mapping.

Satellite	Sensor/Level	Acquisition Date	Spatial Resolution	Source
Sentinel-2	MSIL1C	15 November 2018	10m	ESA
Sentinel-2	MSIL1C	04 November 2020	10m	ESA
Sentinel-2	MSIL1C	30 October 2022	10m	ESA

ESA - European Space Agency

3.2 LULC CLASSIFICATION

The methodology used in the study revolves around LULC classification and LULC modelling. LULC maps are created by classifying pre-processed Sentinel-2 images into four classes: water, built-upareas, barren land, and green infrastructure (Fig.2). This was done using the supervised classification method, the maximum likelihood classifier. The accuracy of each LULC is evaluated using the kappa statistic and an error matrix. LULC modelling involves change analysis, determination of driving factors for transition potential using artificial neural networks based on Cellular automata, and model validation for accuracy using reference LULC through visual and statistical methods, i.e., kappa statistics. Lastly, change modelling using a Markov chain is used to predict future scenarios for 2030.

3.2.1 CLASSIFICATION SCHEME AND TRAINING DATA

For the present study Four LULC classes were chosen based on USGS Anderson Level I system, they are; water bodies, green infrastructure (vegetation/forests), built-up (residential/commercial/industrial), and barren land (exposed soil/rock). Training samples (n=500 per class per year) were generated via stratified random sampling within visual interpretation polygons, and were validated against high-resolution Google Earth Pro-imagery (2022 vintage) and field reconnaissance data, where available.

3.2.2 SUPERVISED MAXIMUM LIKELIHOOD CLASSIFICATION

The maximum likelihood classifier (MLC)—a parametric supervised algorithm assuming multivariate normal distribution of class spectral signatures—was applied in SCP/QGIS. MLC assigns pixels to classes based on Bayesian probability, incorporating class co-variance matrices derived from training data:

$$P(Ck \mid x) = \frac{p(x|Ck)P(Ck)}{\sum j=1mp(x|Cj)P(Cj)} \quad \text{------ (1)}$$

where P(Ck|x) is the posterior probability of class kgiven spectral vector x, p(x|Ck) is the class-conditional likelihood, and P(Ck) is the prior probability. Post-classification refinements included majority filtering (3×3 kernel) to reduce salt-and-pepper noise and manual editing of obvious misclassifications (e.g., shadows as water).

3.2.3 ACCURACY ASSESSMENT

Classification accuracy was calculated using 200 autonomous validation points per class per year, stratified by class area. Overall accuracy (OA), producer's accuracy (PA), user's accuracy (UA), and kappa coefficient (κ) were computed from confusion matrices:

$$\kappa = \frac{OA-E}{1-E} \quad \text{---- (2)}$$

Where E is expected agreement by chance, kappa thresholds >0.80 indicate strong agreement.

Where OA is the overall accuracy and E is the expected agreement by chance.

Equation 3 — Expected Agreement (E), derived from the confusion matrix

E = [Σi (xi+ × x+i)] ⁄ N2 --(3)

Where xi+ is the row total (pixels classified as class i), x+i is the column total (reference pixels in class i), N is the total number of validation points, and the summation runs over all r classes (i = 1, …, r).

3.3 URBAN GROWTH MODELLING

3.3.1 MODEL FRAMEWORK: MLP-MARKOV CHAIN IN LCM

The Land Change Modeler (LCM) v20.0 in IDRISI TerrSet was used to implement a hybrid MLP-Markov CA model for LULC prediction. The workflow comprised: (i) empirical change analysis (2018-2020 → 2020-2022); (ii) MLP-based transition potential mapping; (iii) Markov chain quantification of transition areas; and (iv) CA integration for spatial allocation.

3.3.2 TRANSITION POTENTIAL MODELLING

Two key transitions to built-up were modelled: green infrastructure → built-up, and barren land → built-up, identified as dominant from change analysis. MLP neural networks (feed-forward, back propagation) estimated transition potentials using three proximity-based drivers: (1) Distance to nearest road (2022 OSM network, Euclidean distance), (2) Distance to existing built-up (2022 LULC class), (3) Distance to ORR alignment. Training used 10,000 pixels per transition (50% training/50% validation), with 10,000 iterations and RMSE stopping criterion. MLP architecture: input layer (3 drivers), one hidden layer (12 nodes), sigmoid activation.

3.3.3 MARKOV CHAIN ANALYSIS AND PREDICTION

Markov matrices quantified transition probabilities and areas between 2018-2020 (calibration) and 2020-2022 (projection), using multi-criteria evaluation (MCE). Hard predictions generated categorical 2022 maps; soft predictions produced continuous vulnerability maps (0-1) for validation. Future scenarios (2030, 2040 and 2050) are simulated from validated 2022 maps, extrapolating 2020-2022 transition rates under stationary assumptions.

3.4 MODEL VALIDATION

Simulated 2022 LULC was validated against the observed 2022 using:

- Visual comparison: overlay of simulated vs. reference maps
- Quantitative metrics: three kappa variants—K_standard (class agreement), K_no (quantity agreement), K_location (location agreement).

Thresholds: K_standard>80%, K_no>85%, K_location>85% indicate reliable performance. Area statistics and transition matrices provided supplementary validation. Figure 2 illustrates the integrated workflow. All spatial analyses used the WGS84/UTM Zone 43N projection.

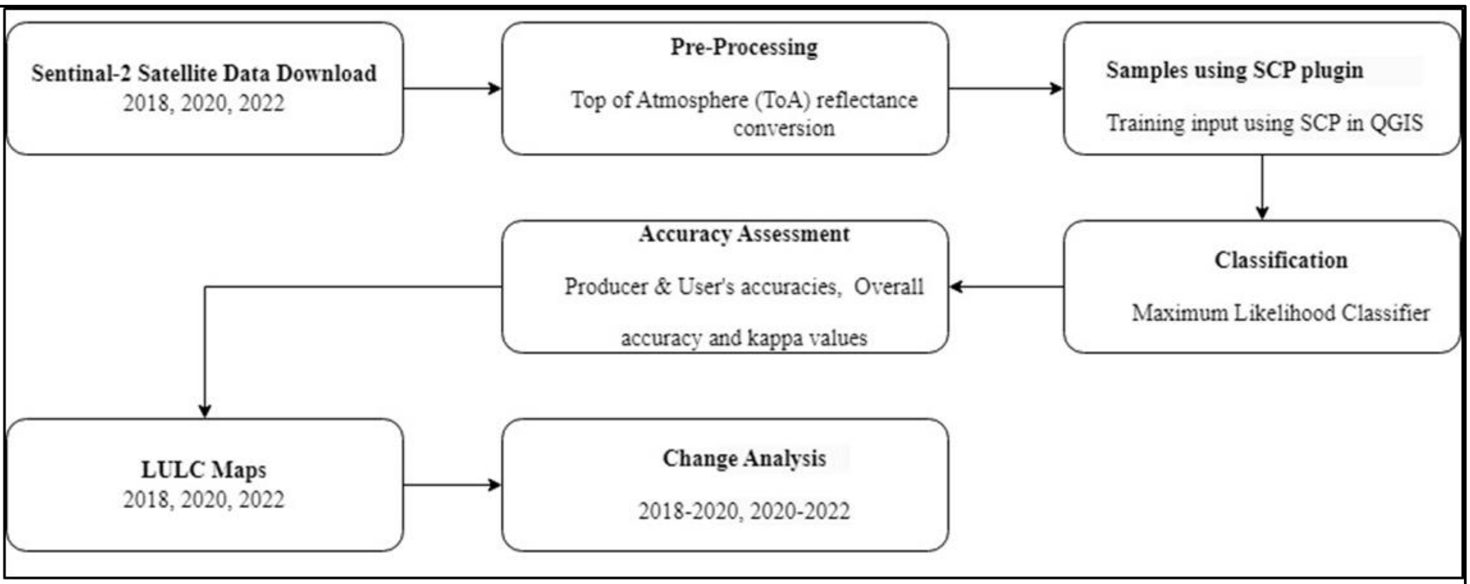

Figure 2(a) Methodological flow chart for Land Use Analysis

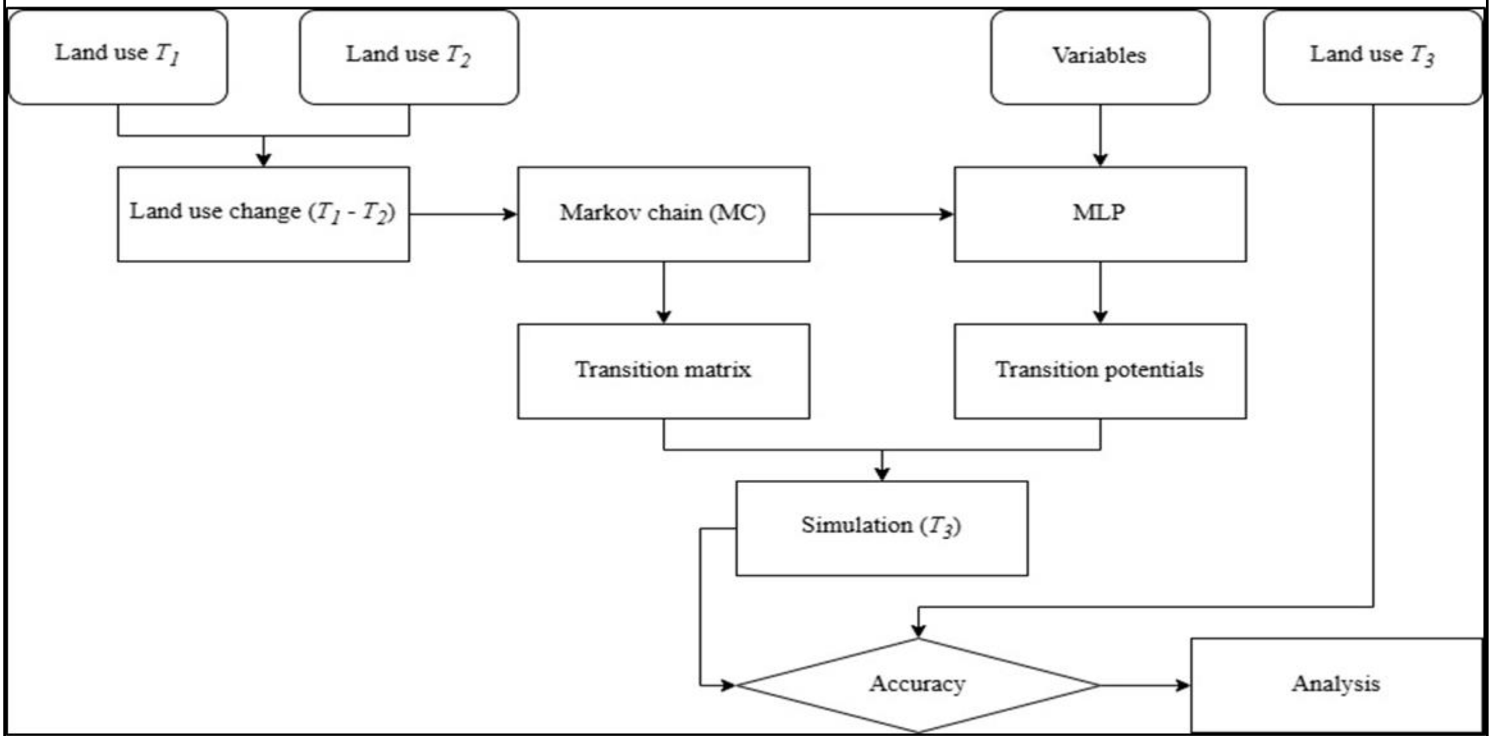

Figure 2(b) Methodological flow chart for Land use simulation using MLP-MC

4. RESULTS AND DISCUSSION

4.1 LULC CLASSIFICATION AND ACCURACY ASSESSMENT

LULC maps for 2018, 2020, and 2022 were generated successfully from Sentinel-2 imagery, delineating four classes: water, green infrastructure, built-up, and barren land (Fig. 3). Classification accuracies were high across all years. Producers' and users' accuracies for the built-up class ranged from 92-96%, confirming robust discrimination of urban features despite spectral similarities with barren land (Table 2). These accuracies align with MLC performance in comparable Sentinel-2 urban studies, where $\kappa > 0.90$ indicates strong agreement beyond chance (Megahed et al., 2015; Talukdar et al., 2020). Minor confusion occurred between green cover and shadows have been addressed using post classification filtering.

Table 2 shows Accuracy assessment class for the years 2018, 2020, and 2022.

	Land Cover Classes			
	Water	Green Infrastructure	Built-up	Barren land
2018				
Producer Accuracy (%)	82.22	97	100	99.96
User Accuracy (%)	100	96.88	99.13	80.07
Kappa	1	0.96	0.98	0.76
2020				
Producer Accuracy (%)	63.94	81.02	100	99.93
User Accuracy (%)	100	97.42	99.77	76.53
Kappa	1	0.97	0.99	0.72
2022				
Producer Accuracy (%)	88.52	92.78	100	88.36
User Accuracy (%)	100	95.30	98.37	89.17
Kappa	1	0.94	0.96	0.87

4.2 SPATIO-TEMPORAL LULC DYNAMICS (2018-2022)

Built-up area expanded substantially from 844.36 km^2 (57.81%) in 2018 to 948.95 km^2 (64.97%) in 2022, a net gain of 104.59 km^2 or 7.16% of total ORR area (Table 3). Green infrastructure declined sharply from 301.04 km^2 (20.61%) to 173.45 km^2 (11.87%), losing 127.59 km^2 primarily to built-up conversion. Barren land fluctuated (287.60 km^2 to 299 km^2), while water bodies showed minor variation (27.66 km^2 to 39.27 km^2).

Transition analysis revealed green infrastructure → built-up (8.74% of total area) and barren land → built-up (2.3%) as dominant shifts, concentrated along ORR corridors and radial roads (Fig. 4a-b). This pattern mirrors rapid peri-urban conversion observed in other Indian megacities (Ramachandra et al., 2012; Aithal et al., 2013).

Table 3 (a) LULCC statistics in (Km^2) from 2018 to 2020, (b) LULCC statistics from 2020 to 2022.

A. Classes	2018	2020	Change	2018 (%)	2020 (%)	Change (%)
Water	2,76,64,500	2,72,39,800	-4,24,700	1.89	1.86	-0.03
Green Infrastructure	30,10,44,300	25,73,25,500	-4,37,18,800	20.61	17.62	-2.99
Built-up	84,43,62,000	89,96,23,100	5,52,61,100	57.81	61.59	3.78
Barren land	28,76,04,200	27,64,86,500	-1,11,17,700	19.69	18.93	-0.76
B. Classes	**2020**	**2022**	**Change**	**2020 (%)**	**2022 (%)**	**Change (%)**
Water	2,72,39,800	3,92,73,100	1,20,33,300	1.86	2.69	0.82
Green Infrastructure	25,73,25,500	17,34,49,600	-8,38,75,900	17.62	11.87	-5.74
Built-up	89,96,23,100	94,89,48,000	4,93,24,900	61.59	64.97	3.38
Barren land	27,64,86,500	29,90,03,800	2,25,17,300	18.93	20.47	1.54

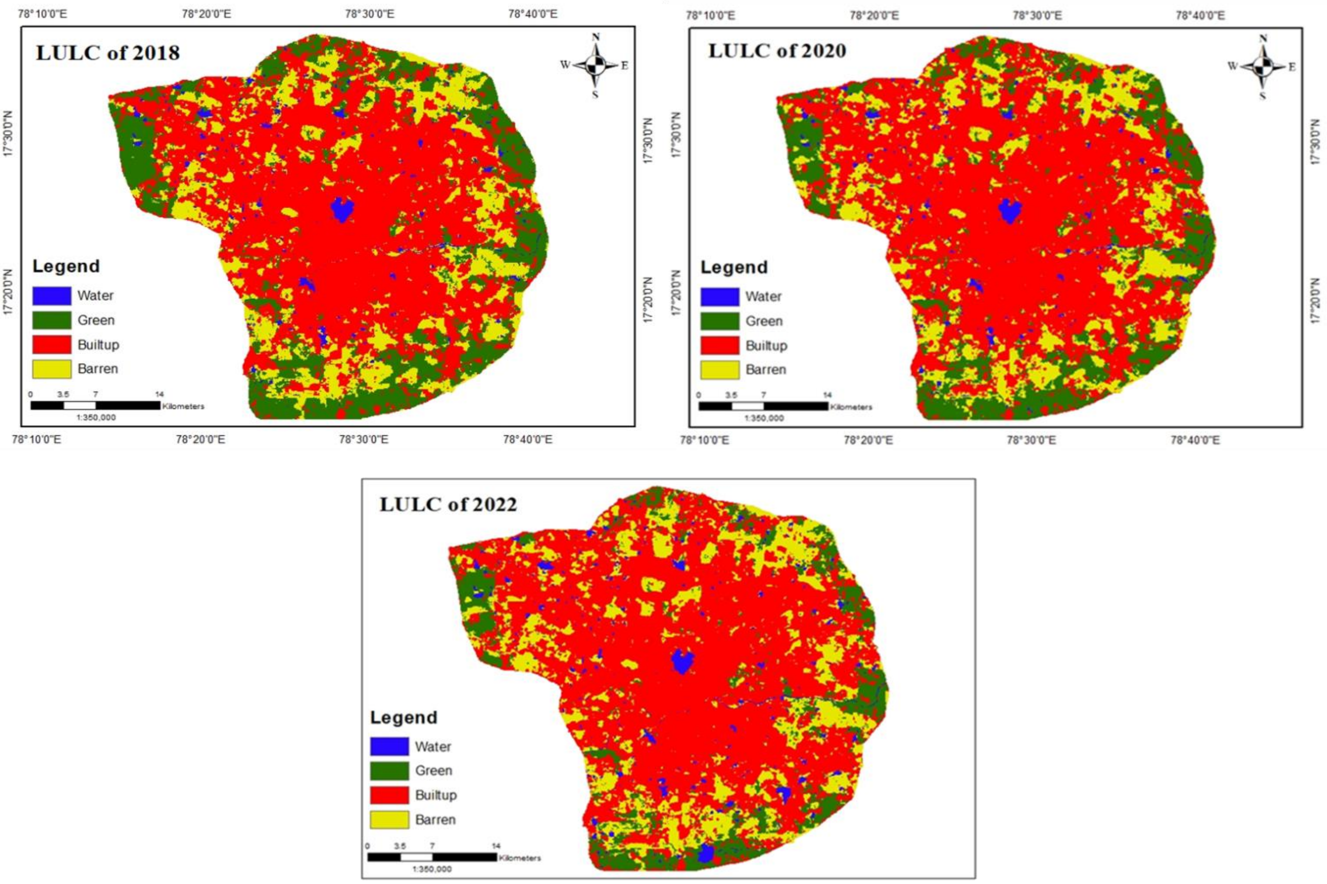

Figure 3 Landuse maps used in the study region using Sentinel 2 imagery (2018, 2020 and 2022).

4.3 MODEL IMPLEMENTATION USING MLP-MC

4.3.1 TRANSITION POTENTIAL MODELLING AND DRIVING FORCES DETERMINATION

The figure (Fig. 4(a)) shows the net change and its contributors in built-up from 2018 to 2020. The two key transitions in the model, from barren land to urban and also from green infrastructure to urban, were highlighted by the LULC results as significant changes. The driving reasons behind both transitions to urban regions were the same, according to a visual analysis of the urban spatial trend, which showed that the chosen predictor variables distance to roads and urban areas affected both transitions. It was found that the chosen factors were significant and worthy of consideration. The major contributors to built-up (Fig. 4(b)) show that green infrastructure and barren land are the classes most likely to be transitioning to urban settlements. Therefore, the model learns the same pattern to further simulate the situation in future years. The model parameters were then set to achieve the best performance and output. Each class sample size is set to 10,000 pixels, of which 50% (5000) were used as training input and the other 50% for sub-model validation. The stopping criteria for the sub-modeL WERE SET TO 10,000 ITERATIONS, with proximity to roads and existing built-up emerging as the strongest predictors with transition potential maps showing elevated values near roads and existing built-up areas, consistent with variables' expected role as growth drivers. These spatial trends validate the driver selection, as urban expansion in Hyderabad correlates strongly with transport accessibility ($r^2 > 0.75$ in similar studies; Maithani, 2009; Guo et al., 2020).

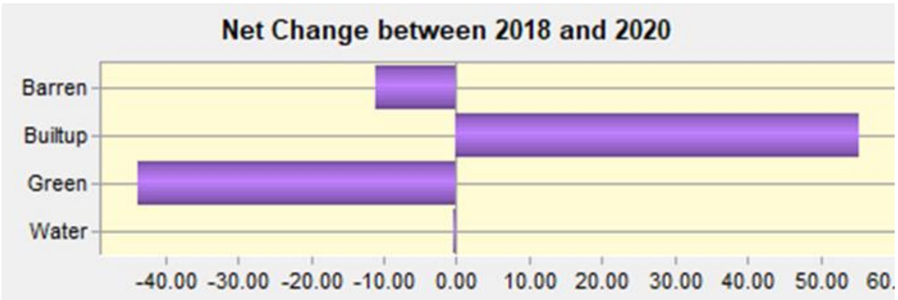

Figure 4(a) Net change between 2018 and 2020

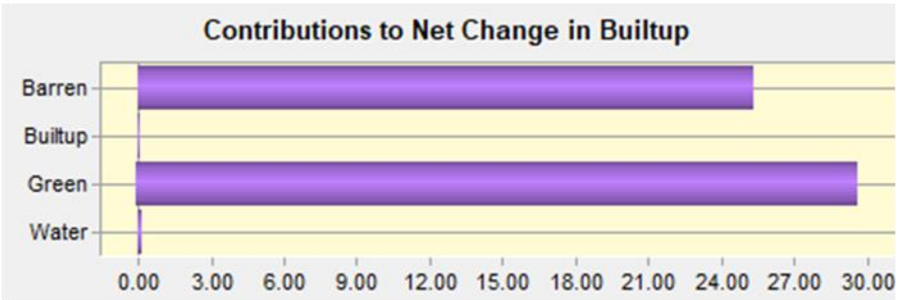

Figure 4(b) Contributions to Net change in built-up from 2018 and 2020

Spatial trends in changes in the driving factors describe the probability of transition from each particular class to other classes. Figure (Fig. 5(a)) shows the cubic trend of the green infrastructure to built-up class, red

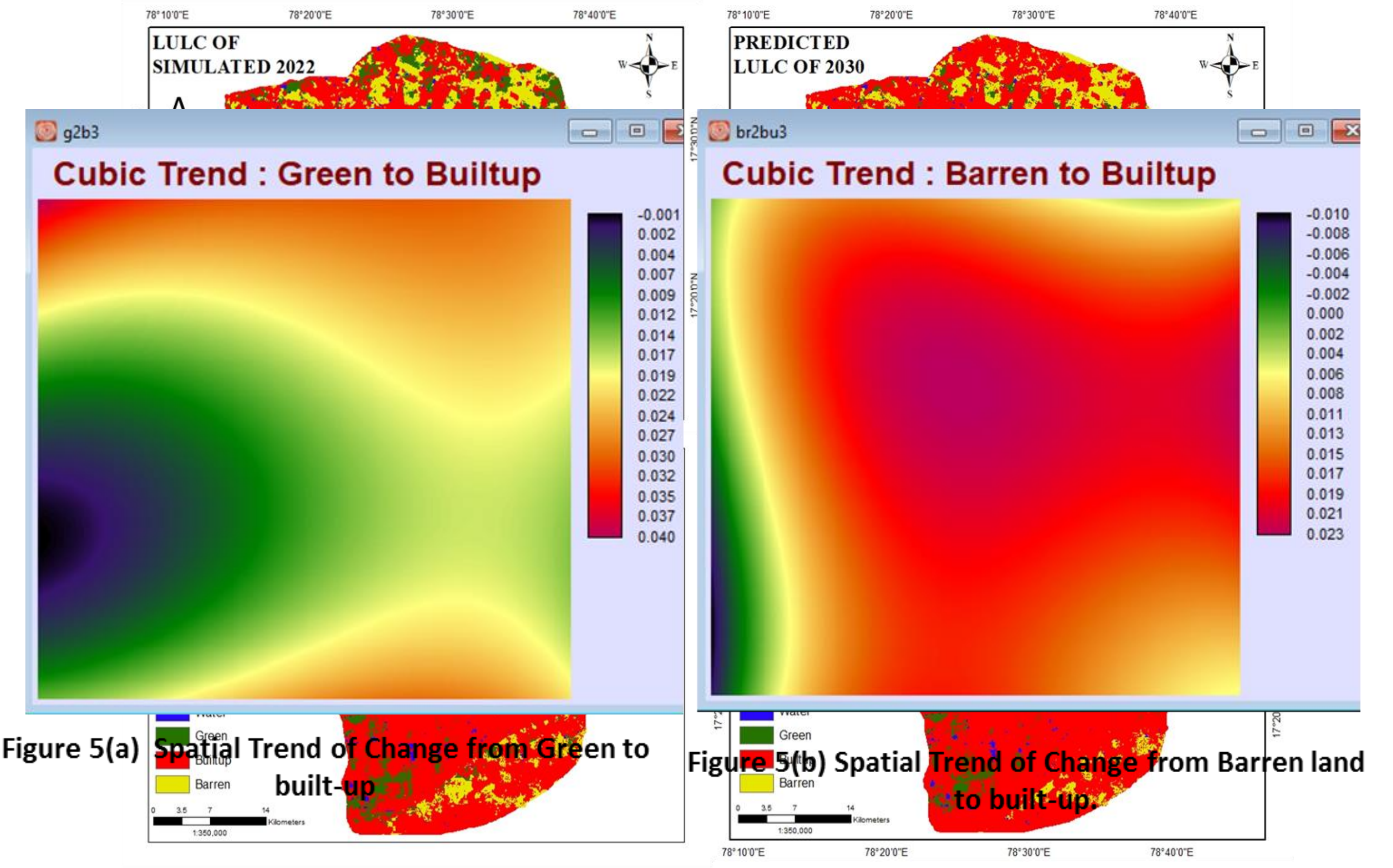

Figure 5(a) Spatial Trend of Change from Green to built-up

Figure 5(b) Spatial Trend of Change from Barren land to built-up.

Figure 6 Simulated LULC for the year 2022 and Predicted LULC for the year 2030, 2040 and 2050.

indicating higher chances of transition to blue representing least chance of probability. Similarly, the figure (Fig. 5(b)) shows the cubic trend of barren land to built-up class.

4.3.2 MODEL VALIDATION: SIMULATED VS. OBSERVED 2022 LULC

The MLP-MC model accurately simulated 2022 LULC from a 2020 baseline, with a visual overlay showing strong spatial congruence in built-up expansion patterns (Fig. 6a). Quantitative validation yielded K_standard = 84.98%, K_no = 87.83%, and K_location = 89.01%, all exceeding acceptability thresholds and confirming reliable quantity, class, and location agreement. Built-up prediction accuracy reached 98.6%, with minimal over-/under-prediction (±1.2 km²).

These kappa values surpass many CA-Markov validations in literature (K_standard ~80%; Jokar et al., 2013; Mansour et al., 2020), attributable to high-quality Sentinel-2 inputs and contextually relevant drivers.

To predict a future scenario for 2022, LCM considers the driving factors, transition potential maps, and change rates derived from the change analysis. The transition potential matrix for 2022 shows that the biggest contributors to built-up were green and barren land, with 11.95% and 11.28% changing to urban areas.

The model is then run to simulate LULC for 2022. The simulated LULC of 2022 (Fig. 6(a)) is visually similar to the LULC of 2022. The statistics for both LULCs are given in Table 3, which shows the prediction accuracy and the % difference between simulation and reality, which are very close. The prediction accuracy of the built-up class was 98.6% which shows the transition sub-model was trained to perfection and can be utilized for further prediction.

4.3.3 FUTURE LULC PROJECTIONS (2030-2050)

To estimate the 2030 LULC map, the changes between 2018 and 2022 were modeled using the actual LULC maps. Figure 6 (b)(c)(d) shows the estimated urban settlements in the year 2030, 2040, and 2050. Urban expansion has boomed over the start of the previous decade and the modelling results confirm that it will continue to increase in 2030. By 2030, model projections indicate urban areas will expand to 1,135.46 km², covering approximately 77.73% of the region. This extensive unplanned growth poses a significant threat to the ecological system, with the potential to degrade green infrastructure and increase barren land. Consequently, the city's cultural heritage is at risk, particularly given the anticipated population surge in the capital. The future LULC projections are subjected to uncertainties; this may be considered as limitation of the present work.

5. CONCLUSIONS

This study demonstrates that integrating high resolution Sentinel 2 imagery with a multilayer perceptron–Markov chain (MLP–MC) framework is an effective approach for analyzing and predicting LULC dynamics in the Hyderabad ORR region. The classification achieved high overall accuracies of 94.8%, 94.7% and 96.3% with kappa coefficients of 0.92, 0.90, and 0.93 for 2018, 2020, and 2022, respectively, while the urban growth model yielded K_standard = 84.98%, K_no = 87.83% and K_location = 89.01%, indicating reliable quantity and location agreement between simulated and observed 2022 LULC. Results show rapid built up expansion from 844.36 km² (57.81%) in 2018 to 948.95 km² (64.97%) in 2022, largely at the expense of green infrastructure, with projections indicating that built up area will reach about 1135.46 km² (77.73%) by 2030 and exceed 90% of the ORR region by 2050, posing serious risks to ecological integrity, flood regulation, and thermal comfort in this semi-arid metropolitan setting. Furthermore, the LULC projections for 2030 and 2050 are subjected to uncertainty stem from different sources. This may be considered as limitation of the present work.

Methodologically, the work is significant because it operationalizes and validates an MLP–MC workflow that captures nonlinear proximity effects (e.g., distance to roads and existing built up areas) more effectively than conventional CA–Markov models, using freely available Sentinel 2 data and open geospatial platforms (QGIS, TerrSet). This provides a replicable template for urban growth modelling in other rapidly urbanizing Indian and South Asian cities with similar data and institutional capacities, and strengthens geospatial competencies within civil engineering and planning education at institutions such as Osmania University. From a policy perspective, the Hyderabad specific transition matrices and scenario maps provide evidence for HMDA and GHMC to prioritize green belt preservation along the ORR, promote vertical densification instead of horizontal sprawl, and integrate LULC projections into flood and heat risk sensitive zoning, aligning with SDG 11 (Sustainable Cities) and national disaster risk management priorities.

However, several limitations should be acknowledged. The transition potential models relied on a limited set of proximity based driving factors (distance to roads, built up, ORR), omitting socio economic drivers (e.g., land values, employment centres) and biophysical variables (e.g., slope, soil), which can influence urban growth pathways (Guo et al., 2020). The use of maximum likelihood classification, while performing well here, assumes Gaussian class distributions and may be outperformed by non-parametric machine learning algorithms such as random forest or support vector machines in complex urban environments (Talukdar et al., 2020). Furthermore, future scenarios for 2030, 2040, and 2050 are based on the assumption of stationary transition probabilities derived from 2018–2022 trends, and thus do not explicitly account for possible policy interventions, infrastructure megaprojects, economic shocks, or climate variability that could alter urbanization trajectories. Spatial resolution (10 m) and the lack of systematic field validation also introduce some uncertainty in class boundaries and fine scale intra urban patterns.

Building on these findings, future research should expand the driver set to include dynamic socio economic datasets (e.g., census indicators, land price proxies, nighttime lights) and additional environmental variables, thereby enhancing the explanatory and predictive power of MLP models (Zhang, 2016). Comparative experiments using advanced classifiers and deep learning architectures, such as random forests, gradient boosting, and convolutional neural networks, could be undertaken to improve discrimination between urban sub classes and informal settlements. Scenario based modelling that integrates alternative policy options—such as strict green buffer implementation, transit oriented development, or zoning reforms—would shift the analysis from “business as usual” projections to normative planning support tools (Ramachandra et al., 2012). Additionally, fusing Sentinel 2 with Sentinel 1 SAR time series could enable more frequent, all weather monitoring, while coupling LULC projections with hydrological and urban climate models would allow explicit quantification of impacts on Musi River flooding, runoff regimes, and urban heat islands, thereby directly informing resilience oriented infrastructure and land use planning in Hyderabad and comparable cities.

Acknowledgements

We would like to express our gratitude appropriate data sources QGIS, Sentinel-2 satellite Imagery (European Space Agency). We would like to thank anonymous reviewers for their useful comments for the improvement of the manuscript.

Conflicts of Interest: The authors declare no conflicts of interest.

Informed Consent Statement: Not Applicable

Author Contributions: SHA carried the analysis, SK conceptualized the work, HG helped in drafting the manuscript, AP revised the text and suggestions.

8 REFERENCES

1. Anderson, J. R., et al. (1976). A land use and land cover classification system for use with remote sensor data. Geological Survey Professional Paper No. 964, U.S. Government Printing Office, Washington DC.

2. Aithal, B. H., Vinay, S., Durgappa, S., & Ramachandra, T. V. (2013). Modeling and Simulation of Urbanisation in Greater Bangalore, India. National Spatial Data Infrastructure Conference, 1–7.

3. Courage, K., Masamu, A., Bongo, A., & Munyaradzi, M. (2009). Rural sustainability under threat in Zimbabwe—simulation of future land use/cover changes in the Bindura district based on the Markov–cellular automata model. Applied Geography, 29, 435–447.

4. Guan, D., Li, H., Inohae, T., Su, W., Nagaie, T., & Kazunori. (2011). Modeling urban land use change by the integration of cellular automaton and Markov chain. Ecological Modelling, 222, 3761–3722.

5. Guo, A., Zhang, Y., & Hao, Q. (2020). Monitoring and Simulation of Dynamic Spatiotemporal Land Use/Cover Changes. Complexity, 2020. https://doi.org/10.1155/2020/3547323

6. Jeanne, E., Karen, P., & Elizabeth, K. (2002). Techniques for mapping suburban sprawl. Photogrammetric Engineering & Remote Sensing, 63(9), 913–918.

7. Jieli, C., Manchun, L., Yongxue, L., Chenglei, S., & Wei, H. (2010). Extract residential areas automatically by New Built-up Index. Proceedings of Geoinformatics, 1–5.

8. Jokar, J. A., Helbich, M., Kainz, W., & Darvishi, B. A. (2013). Integration of Logistic Regression and Markov Chain Models to Simulate Urban Expansion. International Journal of Applied Earth Observation and Geoinformation, 21, 265–275.

9. Kumar, A.K., Rakesh, C.J. and Lokanath, S., 2025. Appraising the Degrees of Sprawl, Freedom and Goodness of Urban Growth Detection Using Geoinformatics Approach-A Study of Tumkur City in Karnataka State, India. Nature Environment & Pollution Technology, 24. https://doi.org/10.46488/NEPT.2024.v24iS1.005

10. Khawaldah, H. A., Farhan, I., &Alzboun, N. M. (2020). Simulation and prediction of land use and land cover change using GIS, remote sensing and CA-Markov model. Global Journal of Environmental Science and Management, 6(2), 215–232.

11. Lillesand, M. T., Kiefer, W. R., & Chipman, W. J. (2004). Remote Sensing and Image Interpretation (5th ed.). John Wiley & Sons.

12. Maithani, S. (2009). A neural network based urban growth model of an Indian city. Journal of the Indian Society of Remote Sensing, 37(3), 363–376.

13. Mansour, S., Al-Belushi, M., & Al-Awadhi, T. (2020). Monitoring land use and land cover changes in the mountainous cities of Oman using GIS and CA-Markov modelling techniques. Land Use Policy, 91, 104414.

14. Megahed, Y., Cabral, P., Silva, J., & Caetano, M. (2015). Land cover mapping analysis and urban growth modelling using remote sensing techniques in Greater Cairo Region, Egypt. ISPRS International Journal of Geo-Information, 4(3), 1750–1769.

15. Pathy, A. C., & Panda, G. K. (2012). Modeling Urban Growth in Indian Situation—A Case Study of Bhubaneswar City. International Journal of Scientific & Engineering Research, 3(6), 1–7.

16. Ramachandra, T. V., & Bharath, H. A. (2012a). Spatio-Temporal Pattern of Landscape Dynamics in Shimoga, Tier II City, Karnataka State, India. International Journal of Emerging Technology and Advanced Engineering, 2(9), 563–576.

17. Ramachandra, T.V, Bharath H. Aithal and D.S. Durgappa (2012b) "Insights to urban dynamics through landscape spatial pattern analysis", International Journal of Applied Earth Observation and Geoinformation, vol.18, p. 329-343.

18. Soffianian, A., Nadoushan, M., Yaghmaei, L. A., &Falahatkar, S. (2010). Mapping and Analyzing Urban Expansion Using Remotely Sensed Imagery in Isfahan, Iran. World Applied Sciences Journal, 9(12), 1370–1378.

19. Sudhira, H. S., Ramachandra, T. V., & Jagadish, K. S. (2004). Urban sprawl: Metrics, dynamics and modelling using GIS. International Journal of Applied Earth Observation and Geoinformation, 5, 29–39.

20. Talukdar, S., Singha, P., Mahato, S., Shahfahad, Pal, S., Liou, Y.-A., & Rahman, A. (2020). Land-use land-cover classification by machine learning classifiers for satellite observations—A review. *Remote Sensing*, *12*(7), 1135. https://doi.org/10.3390/rs12071135

21. Xu, C., Xiao, Y. S., & Ping, Z. A. (2013). Evaluation of Spatiotemporal Dynamics of Simulated Land Use/Cover in China Using a Probabilistic Cellular Automata-Markov Model. Pedosphere, 23(2), 243–255.

22. Wang, H., He, S., Liu, X., Dai, L., Pan, P., Hong, S., & Zhang, W. (2014). Simulating urban expansion using a cloud-based cellular model: A case study of Jiangxia, China. Landscape and Urban Planning, 110, 99–112.

23. Weng, Q. (2001). A remote sensing–GIS evaluation of urban expansion and its impact on surface temperature in the Zhujiang Delta, China. International Journal of Remote Sensing, 22(10), 1999–2014.

24. Zhang, X. (2016). Urban Growth Modeling Using Neural Network Simulation: A Case Study of Dongguan City, China. Journal of Geographic Information System, 8(3), 317–328.